

# Numerical Study on Low Pressure Inductively Coupled Plasma Sources for Nanocrystalline Diamond Deposition

Katsuyuki Okada\*, Shojiro Komatsu, and Takamasa Ishigaki  
Advanced Materials Laboratory, National Institute of Materials Science,  
1-1 Namiki, Tsukuba, Ibaraki 305-0044, Japan; okada.katsuyuki@nims.go.jp

Numerical study on low pressure inductively coupled plasma (ICP) used for nanocrystalline diamond deposition has been performed with direct simulation Monte Carlo (DSMC) method and electron Monte Carlo simulation. Spatial distributions of electron density, electron temperature, and plasma potential are obtained. The electron energy distribution functions (EEDFs) are compared with the experimental results obtained with a Langmuir probe previously. The EEDFs of an Ar and a CH<sub>4</sub>/H<sub>2</sub> plasma obtained from the simulation agree well with the measured data. The calculated EEDF of a CH<sub>4</sub>/H<sub>2</sub> plasma at 50 mTorr exhibits a hump around 6 eV, which corresponds to a hump around 6 eV in the measured EEDF at the same pressure. It can be attributed to the resonant peak of the vibrational excitation cross section of CH<sub>4</sub> molecule.

## 1. Introduction

We have applied a low pressure inductively coupled plasma (ICP) to deposit nanocrystalline diamond [1]. The sp<sup>2</sup>/sp<sup>3</sup> bondings of the nanocrystalline diamond were evaluated with Raman spectroscopy [2] and electron energy loss spectroscopy [3]. Langmuir probe and mass spectrometric measurements were performed to characterize the ICP [4,5]. We obtained plasma parameters {electron density (N<sub>e</sub>), electron temperature (T<sub>e</sub>), and plasma potential (V<sub>p</sub>)}, electron energy distribution functions (EEDFs), and ion energy distributions (IEDs). For better understanding of the ICP, we need a theoretical investigation such as modeling or numerical simulation. Economou et al. [6] used the direct simulation Monte Carlo (DSMC) method to demonstrate reactive neutral and ion flow in an ICP reactor. Nanbu et al. [7] also used the electron Monte Carlo method for obtaining the production rate of radicals. Takekida and Nanbu [8] reported the EEDFs of capacitively coupled Ar plasmas using particle-in-cell/Monte Carlo (PIC/MC) method.

In this study, we report on the numerical simulation of the ICP used for nanocrystalline diamond deposition using DSMC method and electron Monte Carlo simulation. Spatial distributions of N<sub>e</sub>, T<sub>e</sub>, and V<sub>p</sub> are obtained. The calculated EEDFs are compared with the measured EEDFs.

## 2. Experiment and Simulation

The detailed descriptions of low pressure ICP-CVD system and Langmuir probe measurement were reported previously [1,4]. To be brief, a low pressure ICP was generated in a

growth chamber by applying 13.56 MHz rf powers of 1 kW to a three-turn helical antenna wound around a quartz tube. An Ar or a CH<sub>4</sub>/H<sub>2</sub> (5:75 mixture) plasma was generated at pressures ranging from 10 to 50 mTorr. A Langmuir probe (Smart Probe; *Scientific Systems Inc.*) was utilized to measure plasma parameters and EEDFs.

The procedure of simulation is as follows. The flow, electromagnetic field, and plasma are assumed to be axisymmetric. The height of the reactor is 110 mm. A three-turn helical coil wound around a quartz tube with 40 mm in diameter. The calculation was performed with DSMC method and electron Monte Carlo simulation. Collisions of e-H, e-H<sub>2</sub>, e-CH<sub>4</sub>, e-CH<sub>3</sub>, e-CH<sub>2</sub>, and e-CH are considered in a CH<sub>4</sub>/H<sub>2</sub> plasma.

Surface reactions of radicals play a critical role in determining the concentrations and distributions of ions and radicals in a reactive plasma such as CH<sub>4</sub>/H<sub>2</sub> plasma. The sticking of CH<sub>3</sub>, CH<sub>2</sub>, and CH radicals on the surface are taken into consideration in the calculation. The sticking coefficients of CH<sub>4</sub>, CH<sub>3</sub>, and CH<sub>2</sub> radicals are referred to 1.0X10<sup>-4</sup>, 1.0X10<sup>-3</sup>, and 3.0X10<sup>-2</sup> in the previous reports [9-11].

## 3. Results and Discussion

Figures 1(a) and 1(b) show the N<sub>e</sub> and T<sub>e</sub> of an Ar plasma at 50 mTorr, respectively. The N<sub>e</sub> is concentrated near the rf antenna, and the T<sub>e</sub> has a doughnut-shape distribution near the rf antenna. Figure 2(a) and 2(b) show the density of Ar<sup>+</sup> and Ar\*, respectively. While the former has a similar distribution to the N<sub>e</sub>, the latter spreads toward the growth chamber.

The N<sub>e</sub> and T<sub>e</sub> of a CH<sub>4</sub>/H<sub>2</sub> plasma at 50 mTorr

are shown in Fig. 3(a) and 3(b), respectively. The  $N_e$  is concentrated near the rf antenna similar to that of Ar plasma. The  $T_e$  is high along the quartz tube, which is different from that of Ar plasma. The density of  $H^+$ ,  $CH_3^+$ ,  $H^*$ , and  $CH_3^*$  are shown in Fig. 4(a), 4(b), 4(c), and 4(d), respectively. While the ion distributions are concentrated near the rf antenna, the radical distributions spread into the growth chamber. The distributions strongly depend on each radical.

Figure 5(a) shows the measured EEDF of an Ar plasma at 50 mTorr (closed circles) and the calculated one at the same pressure (open circles). The each EEDF is nearly a straight line, which means that the electron energy has a Maxwellian distribution. Although the calculated EEDF above 10 eV slightly deviates from a straight line, it is consistent with the measured EEDF.

Figure 5(b) shows the measured EEDF of a  $CH_4/H_2$  plasma at 50 mTorr (closed circles) and the calculated one at the same pressure (open circles). They are different from the EEDF of an Ar plasma at the same pressure. There is a hump around 6 eV in both measured and calculated EEDF. Turner and Hopkins [12] reported the unusual structure of the EEDF. They found a dip around 4 eV in the EEDF of a  $N_2$  plasma, which is interpreted as the electric absorption of  $N_2$  molecule corresponding to the resonant peak of the vibrational excitation cross section. In the  $CH_4$  vibrational excitation cross sections,  $\sigma_{v(1,3)}$  and  $\sigma_{v(2,4)}$  have a peak around 6 eV [13]. Therefore, the hump around 6 eV can be attributed to the electric absorption of  $CH_4$  molecule analogous to the vibrational absorption of 4 eV electrons of the  $N_2$  molecule.

The calculated EEDF of a  $CH_4/H_2$  plasma agrees well with the measured one. Accordingly, the unusual structure around 6 eV in the

calculated EEDF can also be attributed to the resonant peak of the vibrational excitation cross section of  $CH_4$  molecule.

### Acknowledgment

The authors would like to thank Mr. M. Tanaka and T. Takasaki of PEGASUS Software Inc. for their useful advice on the calculation.

### References

- [1] K. Okada, S. Komatsu, and S. Matsumoto, *J. Mater. Res.* **14**, 578 (1999).
- [2] K. Okada, H. Kanda, S. Komatsu, and S. Matsumoto, *J. Appl. Phys.* **88**, 1674 (2000).
- [3] K. Okada, K. Kimoto, S. Komatsu, and S. Matsumoto, *J. Appl. Phys.* **93**, 3120 (2003).
- [4] K. Okada, S. Komatsu, and S. Matsumoto, *J. Vac. Sci. Technol.* **17**, 721 (1999).
- [5] K. Okada, S. Komatsu, and S. Matsumoto, *J. Vac. Sci. Technol.* **21**, 1988 (2003).
- [6] D. J. Economou, T. J. Bartel, R. S. Wise, and D. P. Lymberopoulos, *IEEE Trans. Plasma Sci.* **23**, 581 (1995).
- [7] K. Nanbu, T. Morimoto, and M. Suetani, *IEEE Trans. Plasma Sci.* **27**, 1379 (1999).
- [8] H. Takekida and K. Nanbu, *Jpn. J. Appl. Phys.* **43**, 3590 (2004).
- [9] W. L. Hsu, *J. Appl. Phys.*, **72**, 3102 (1992).
- [10] H. Toyoda, H. Kojima, and H. Sugai, *Appl. Phys. Lett.*, **54**, 1507 (1989).
- [11] H. Kojima, H. Toyoda, and H. Sugai, *Appl. Phys. Lett.*, **55**, 1292 (1989).
- [12] M. M. Turner and M. B. Hopkins, *Phys. Rev. Lett.* **69**, 3511 (1992).
- [13] W. L. Morgan, *Plasma Chem. Plasma Process.* **12**, 477 (1992).

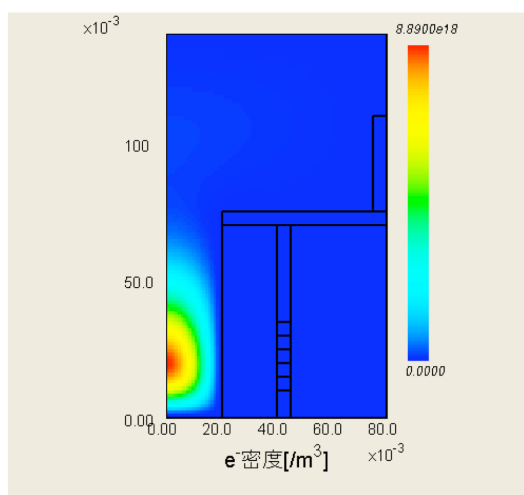


FIG. 1(a) Electron density of Ar plasma

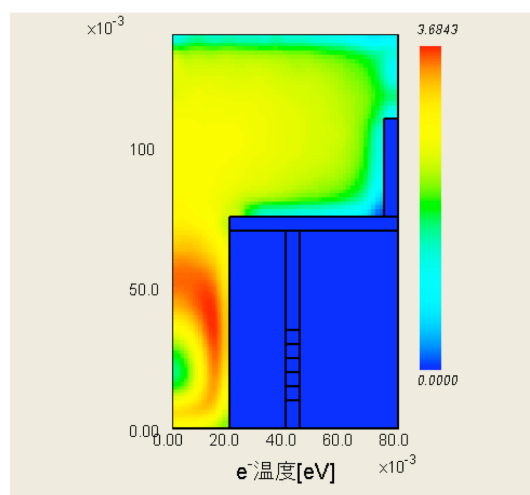


FIG. 1(b) Electron temperature of Ar plasma

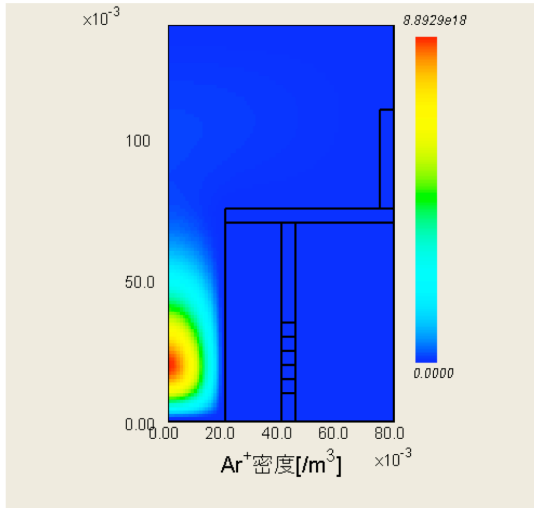


FIG. 2(a) Density of  $\text{Ar}^+$

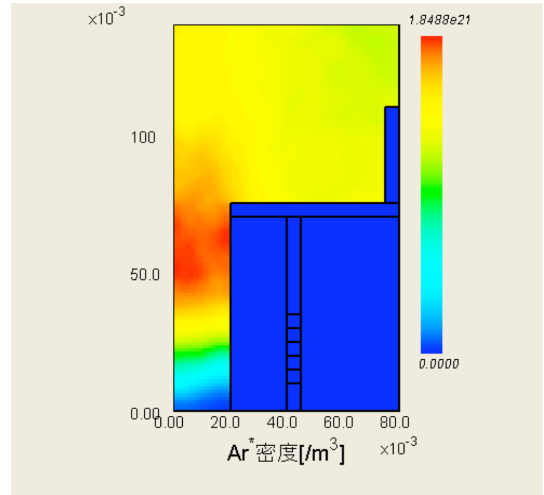


FIG. 2(b) Density of  $\text{Ar}^*$

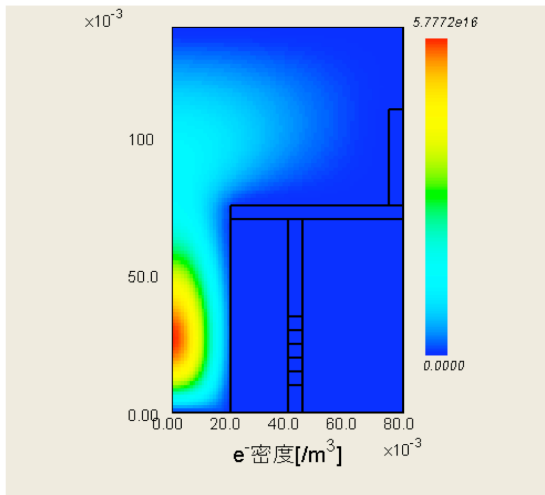


FIG. 3(a) Electron density of  $\text{CH}_4/\text{H}_2$  plasma

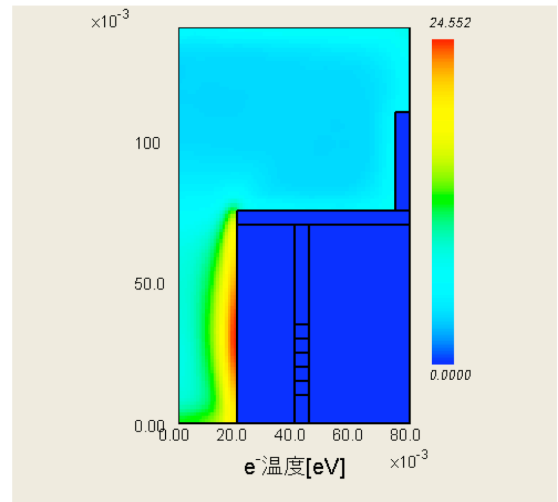


FIG. 3(b) Electron temperature of  $\text{CH}_4/\text{H}_2$  plasma

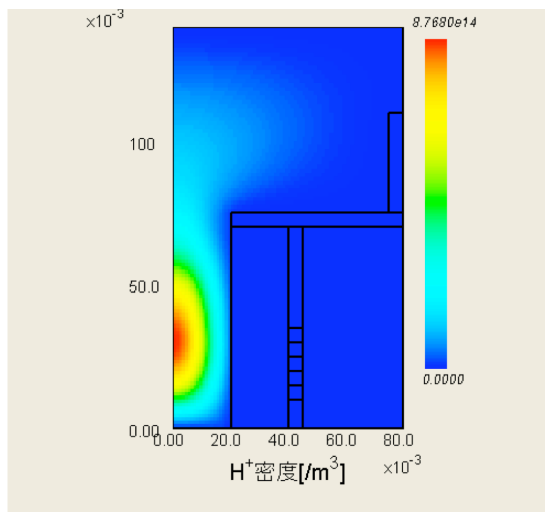


FIG. 4(a) Density of  $\text{H}^+$

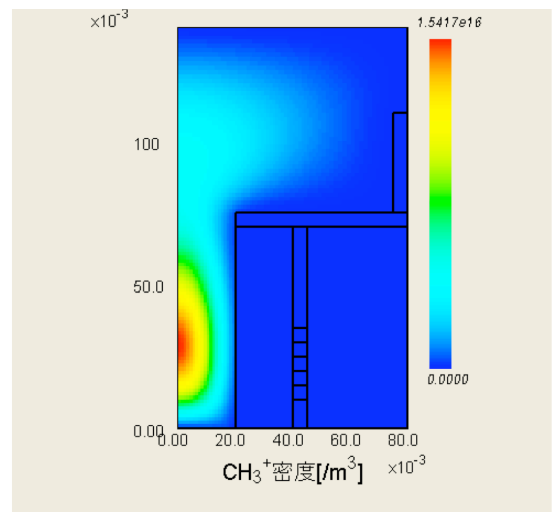


FIG. 4(b) Density of  $\text{CH}_3^+$

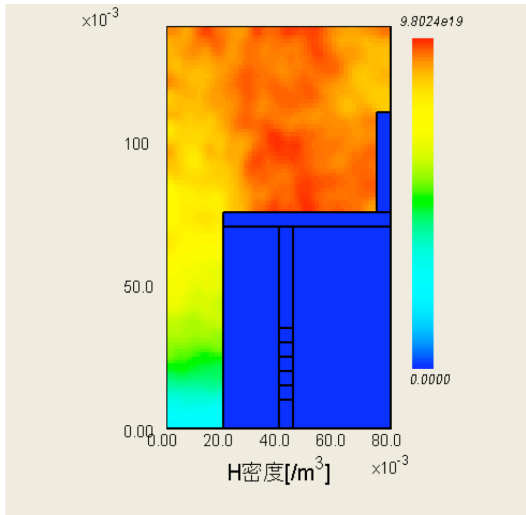


FIG. 4(c) Density of H\*

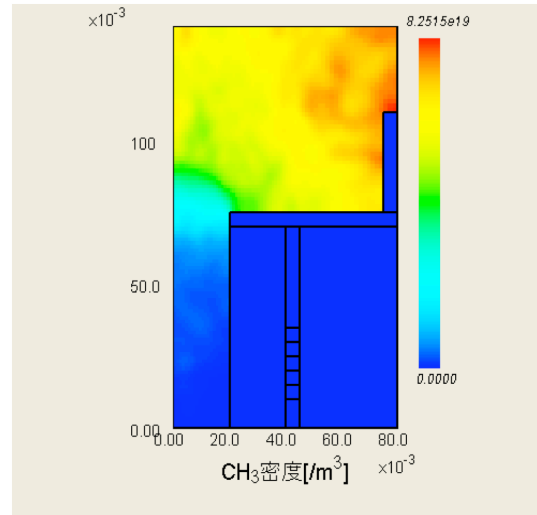


FIG. 4(d) Density of CH<sub>3</sub>\*

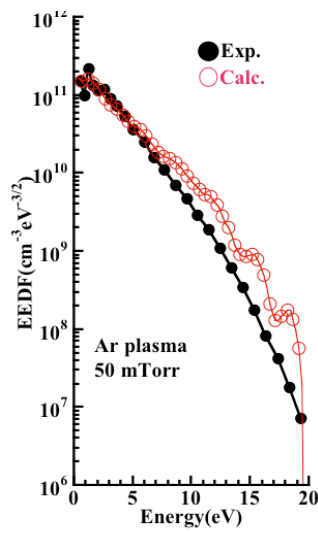


FIG. 5(a) The measured EEDF (closed circles) and the calculated EEDF (open circles) of an Ar plasma at 50 mTorr.

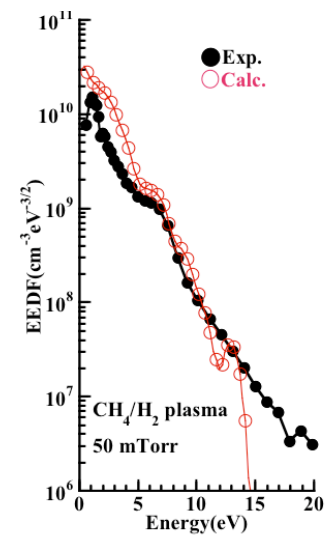


FIG. 5(b) The measured EEDF (closed circles) and the calculated EEDF (open circles) of a CH<sub>4</sub>/H<sub>2</sub> plasma at 50 mTorr.